

SUBSTRUCTURE AND HALO DENSITY PROFILES IN A WARM DARK MATTER COSMOLOGY

PEDRO COLÍN¹ AND VLADIMIR AVILA-REESE²

Instituto de Astronomía, Universidad Nacional Autónoma de México, C.P. 04510, México, D.F., México
AND

OCTAVIO VALENZUELA³

Astronomy Department, New Mexico State University, Box 30001, Department 4500, Las Cruces, NM
88003-0001
Astrophysical Journal, accepted

ABSTRACT

We performed a series of high-resolution collisionless N-body simulations designed to study the substructure of Milky Way-size galactic halos (host halos) and the density profiles of halos in a warm dark matter (WDM) scenario with a non-vanishing cosmological constant. The virial masses of the host halos range from $3.5 \times 10^{12} h^{-1} M_{\odot}$ to $1.7 \times 10^{12} h^{-1} M_{\odot}$ and they have more than 10^5 particles each. A key feature of the WDM power spectrum is the free-streaming length $R_{f,WDM}$ which fixes an additional parameter for the model of structure formation. We analyze the substructure of host halos using three $R_{f,WDM}$ values: 0.2, 0.1, and 0.05 Mpc and compare results to the predictions of the cold dark matter (CDM) model. We find that guest halos (satellites) do form in the WDM scenario but are more easily destroyed by dynamical friction and tidal disruption than their counterparts in a CDM model. The small number of guest halos that we find in the WDM models with respect to the CDM one is the result of a lower guest halo accretion and a higher satellite destruction rate. These two phenomena operate almost with the same intensity in delivering a reduced number of guest halos at $z = 0$. For the model with $R_{f,WDM} = 0.1$ Mpc the number of accreted small halos is a factor 2.5 below that of the CDM model while the fraction of destroyed satellites is almost twice larger than that of the CDM model. The larger the $R_{f,WDM}$ value the greater the size of these two effects and the smaller the abundance of satellites. Under the assumption that each guest halo hosts a luminous galaxy, we find that the observed circular velocity function of satellites around the Milky Way and Andromeda is well described by the $R_{f,WDM} = 0.1$ Mpc WDM model. In the $R_{f,WDM} = 0.1 - 0.2$ Mpc models, the surviving guest halos at $z = 0$ —whose masses are in the range $M_h \approx 10^9 - 10^{11} h^{-1} M_{\odot}$ — have an average concentration parameter $c_{1/5} (= r(M_h)/r(M_h/5))$ which is approximately twice smaller than that of the corresponding CDM guest halos. This difference, very likely, produces the higher satellite destruction rate found in the WDM models. The density profile of host halos is well described by the NFW fit whereas guest halos show a wide variety of density profiles. A tendency to form shallow cores is not evident; the profiles, however, are limited by a poor mass resolution in the innermost regions where shallow cores could be expected.

Subject headings: cosmology:theory — cosmology:dark matter — galaxies: formation — galaxies: halos — methods: numerical

1. INTRODUCTION

Non-baryonic dark matter is an essential ingredient of current inflation-inspired models of cosmic structure formation in the universe. From the point of view of particle physics, there is no obvious preference for any of the predicted dark matter candidates (Colombi, Dodelson, & Widrow 1996), which, according to their rms velocity at the time of their decoupling, can be cold, warm, or hot. From the point of view of structure formation, the most compelling candidate has been the cold dark matter. The CDM scenario for structure formation has successfully accounted for several observational facts, particularly on large scales, without introducing an additional free parameter related to its particle distribution function in phase space. However, on small scales and/or in high-density regions of the universe, the predictions of the CDM models

seem to be in conflict with observations.

One of the potential problems of the CDM scenario is that the predicted number of low-mass halos —where probably dwarf galaxies form— within a Milky Way-size halo, greatly exceeds the observed abundance of satellite galaxies in the Local Group (Klypin et al. 1999, hereafter KKVP99; Moore et al. 1999a; see also Kauffmann et al. 1993). A second problem is that the predicted inner density profiles of CDM halos may disagree with the shallow profiles inferred from the rotation curves of dwarf and low surface brightness galaxies (Moore 1994; Flores & Primack 1994; Burkert 1995; de Blok & McGaugh 1997; Hernández & Gilmore 1998), although the observational data for the latter galaxies are controversial (van den Bosch et al. 1999; Swaters, Madore, & Trewheella 2000; but see Firmani et al. 2000b). High-resolution gravitational lensing maps of

¹colin@astroscu.unam.mx

²avila@astroscu.unam.mx

³ovalenzu@nmsu.edu

a cluster of galaxies have also revealed a soft inner mass distribution in the halo of this cluster (Tyson, Kochanski, & Dell’Antonio 1998). The rotation curve decompositions of normal galaxies and the Tully-Fisher relation obtained in galaxy formation models as well as the dark mass contained within the solar radius in our Galaxy, also point out to dark halos shallower and/or much less concentrated than those predicted by the CDM model (Avila-Reese, Firmani, & Hernández 1998; Navarro 1998; Navarro & Steinmetz 1999; Firmani & Avila-Reese 2000; Mo & Mao 2000). If these shortcomings of the CDM scenario are confirmed with more observational and theoretical data, new alternatives (cosmological and/or astrophysical) have to be explored in order to modify the properties of the mass distribution at small scales.

In a recent burst of papers, explored alternatives include modifications to: either the nature of the dark matter candidate (e.g., Spergel & Steinhardt 2000; Hannestad 1999; Sommer-Larsen & Dolgov 2000; White & Croft 2000; Firmani et al 2000a; Hogan & Dalcanton 2000; Moore et al. 2000; Yoshida et al. 2000; Burkert 2000; Peebles 2000; Hannestad & Scherrer 2000; Riotto & Tkachev 2000), or the generation of the primordial power spectrum (e.g., Kamionkowski & Liddle 1999). More conservative astrophysical mechanisms to overcome the problems mentioned above have also been proposed (e.g., Navarro, Eke, & Frenk 1996; Gelato & Sommer-Larsen 1999; Bullock, Kravtsov, & Weinberg 2000; Binney, Gerhard, & Silk 2000). One possible modification is to go from a CDM scenario to a warm dark matter (WDM) one. The WDM particles (warmons) would suppress the power at small scales by free-streaming out of overdense regions limiting the formation of substructure at scales below the free-streaming scale. At large scales, the structure formation would proceed in a very similar way to that of a CDM model. N-body simulations have shown that indeed large-scale structure in WDM models looks similar to that of a CDM model (Colombi et al. 1996). On the other hand, as Hogan & Dalcanton (2000) noted, the finite phase density of dark halos inferred from observations could be pointing to a non-negligible DM velocity dispersion at the time of structure formation.

Using the Press-Schechter formalism, Kamionkowski & Liddle (1999) have shown that if the CDM power spectrum is filtered at scales corresponding to dwarf galaxies, then the abundance of Milky Way satellites can be reproduced. Recently, White & Croft 2000 reported results from N-body simulations for WDM models at high redshifts. They found that the abundance of $10^{10}h^{-1}M_{\odot}$ halos is reduced by a factor of ~ 5 at $z = 3$ with respect to the CDM model when the power spectrum is filtered at $k \approx 2h \text{ Mpc}^{-1}$. At the same time they showed that the Ly- α power spectrum at this redshift is very similar to that of the CDM model, which is in agreement with observations. This apparent contradictory result is explained by the fact that the collapse of large-scale structures, as they go non-linear, regenerates the initially suppressed small-scale modes in the power spectrum (White & Croft 2000).

These results encourage us to explore in more detail the predictions of WDM N-body simulations at the present epoch. Does the suppression of power at small scales of a WDM model actually eliminate the excessive degree of substructure predicted by the CDM scenario? Are the

WDM halos less concentrated? And if so, do they have a smoother inner mass distribution than their counterpart CDM halos? The main aim of this paper is to give a quantitative answer to the first question. To this end we have carried out high-resolution N-body simulations of Milky Way-size galactic halos in three different WDM models. A host halo of about $2 \times 10^{12} h^{-1}M_{\odot}$ has more than 10^5 particles in the simulations. Since the most successful variant of the CDM models is a flat universe with a non-zero cosmological constant ($\Omega_{\Lambda} = 0.7$ and $h = 0.7$), here we also use this cosmological model but instead of CDM we introduce WDM with the extra free parameter $R_{f,WDM}$: these models will be our Λ WDM models (for economy we drop off the greek letter Λ hereafter when we refer to either CDM or WDM models). We will also address the questions of concentrations and density profiles of dark halos, although the small number of large high-resolved halos and the small range of masses in the simulations constrain our predictions on this subject.

In Section 2 we discuss the WDM models to be explored in this paper. In Section 3 we briefly describe the numerical technique that we used for the simulations. Section 4 is devoted to the analysis and comparison with observations of the circular velocity function of satellites within host halos of Milky Way-sizes. The concentrations and density profiles of the host and satellite halos are presented in Section 5. In Section 6 we discuss some of the results, and summarize of our main conclusions is given in Section 7.

2. THE Λ WDM COSMOLOGICAL MODELS

Several observational tests such as the distribution of galaxies (e.g., Peacock & Dodds 1994), cluster mass estimates (e.g., Carlberg et al. 1996), the determination of the baryon fraction in clusters (e.g., Mohr, Mathiesen, & Evrard 1999), and the evolution of cluster abundance (e.g., Eke et al. 1998) point to a cosmological CDM model with a low matter density, $\Omega_0 \approx 0.3$. This model also successfully accounts for the observationally inferred values of the Hubble constant and the age of the universe. On the other hand, according to a prediction of the inflationary theory, the universe should be flat, i.e. a contribution to the density of the universe from a cosmological constant is necessary if $\Omega_0 \approx 0.3$. It has been inferred recently from observations of high redshift Supernovae that the universe is expanding with positive acceleration (Perlmutter et al. 1999; Riess 1998; Schmidt et al. 1998). Remarkably, the estimated value of the cosmological constant density parameter is in this case $\Omega_{\Lambda} \approx 0.6 - 0.8$. Thus, the most popular cosmological model has become a flat CDM model with a non-vanishing cosmological constant: $\Omega_0 \approx 0.3$, $\Omega_{\Lambda} \approx 0.7$, and $h = 0.7$ (the Hubble constant in units of $100 \text{ km s}^{-1} \text{ Mpc}^{-1}$; this value is consistent with the current observational determinations, e.g., Nevalainen & Roos 1998). Here we will use this cosmological model but instead of CDM we will introduce WDM.

A dark matter particle is usually defined as *hot* or *cold* if at the moment of decoupling from the rest of the cosmic plasma it is relativistic or non-relativistic, respectively (Kolb & Turner 1990). The classic and only example of detected dark matter are the neutrinos. They are hot because they were relativistic at the moment of their decoupling. If the mass of the dark matter candidate is much higher than 1 GeV and the strength of its interactions is

comparable to that of the weak interaction, then it would behave as cold dark matter. The thermal velocities of these particles at the time of structure formation is negligible. In this paper we are interested in a *warm* DM candidate, a thermal relic that at the time of its decoupling was relativistic and whose mass m_W is much higher than that of its hot counterpart. The Cowsik-McClelland bound prohibits any candidate with a mass larger than ~ 15 eV (assuming $\Omega_{WDM} \sim 0.3$ and $h = 0.7$) which decouples when the temperature of the universe was a few MeV (Cowsik & McClelland 1972). Thus, the warmton should decouple earlier than a hot candidate, in an epoch when the total number of degrees of freedom of relativistic particles was certainly very high (Kolb & Turner 1990).

Unlike the CDM case, the small-scale density fluctuations are damped out in a WDM scenario by the free-streaming of DM particles. It is straightforward to compute the comoving free-streaming scale $R_{f,WDM}$ (e.g., Sommer-Larsen & Dolgov 2000):

$$R_{f,WDM} = 0.2 (\Omega_{WDM} h^2)^{1/3} \left(\frac{m_W}{1 \text{keV}} \right)^{-4/3} \text{Mpc}. \quad (1)$$

The WDM scenario was not attractive in the past because of the introduction of the extra free parameter $R_{f,WDM}$, and because particles in the required mass range of ~ 100 eV–1 keV were not particularly compelling. Nevertheless, these arguments are somewhat obsolete nowadays. As mentioned in the introduction, the CDM scenario seems to be in disagreement with observational data at small scales, so that models with extra degrees of freedom might be necessary. On the other hand, light WDM candidates as palatable as the CDM ones are also predicted by particle physics beyond the standard model; one possible example are the right-handed neutrinos (e.g., Colombi, Dodelson, & Widrow 1996).

We have represented the WDM power spectrum by the following expression (Bardeen et al. 1986; see also Sommer-Larsen & Dolgov 2000)

$$P_{WDM}(k) = T_{WDM}^2(k) P_{CDM}(k), \quad (2)$$

where the WDM transfer function is approximated by

$$T_{WDM}(k) = \exp \left[-\frac{k R_{f,WDM}}{2} - \frac{(k R_{f,WDM})^2}{2} \right] \quad (3)$$

and P_{CDM} is the CDM power spectrum which is in turn approximated by the following formula (Klypin & Holtzman 1997):

$$P(k) = \frac{Ak}{(1 - 1.5598k^{1/2} + 47.986k + 117.77k^{3/2} + 321.92k^2)^{2 \times 0.9303}} \quad (4)$$

This power spectrum was obtained by a direct fit to the power spectrum estimated using a Boltzmann code and is normalized to $\sigma_8 = 1.0$, close to the cluster abundance and the 4 yr COBE-DMR normalization. Here σ_8 is the rms of mass fluctuations estimated with the top-hat window of radius $8h^{-1}$ Mpc.

Since our aim is to study the substructure in Milky Way-size halos, we simulate WDM models with three different values of $R_{f,WDM}$ namely 0.2, 0.1, and 0.05 Mpc, for which, according to eq. (1), m_W is 605, 1017 and 1711 eV, respectively. Particle masses of this order were recently proposed with the aim to predict fewer Milky Way satellites than in the CDM scenario (Kamionkowski & Liddle 1999; White & Croft 2000). For a 1 keV particle and for $\Omega_{WDM} \sim 0.3$, the rms velocity of the particles is ~ 2 km/s at $z = 40$ (Hogan & Dalcanton 2000). This velocity is too small to affect the structure of our simulated host halos. We thus do not consider in our initial conditions the thermal component contribution to the velocities of the particles.

3. NUMERICAL SIMULATIONS

A set of high-resolution simulations of Milky Way-size halos (defined as host halos) have been performed using a variant of the Adaptive Refinement Tree (ART) N-body code (Kravtsov, Klypin, & Khokhlov 1997). The ART code achieves high spatial resolution by refining the base uniform grid in all high-density regions with an automated refinement algorithm. This version of the ART code (Klypin et al. 2000) has the ability to handle particles with different mass. This is used to increase the mass and spatial resolution in few selected halos. Following, we describe the way in which the simulations have been carried out.

First, we set the number of mass levels in the mass hierarchy to four in all simulations⁴. Particles are eight times more massive when they pass from one level to the next coarser level. For our selected number of mass levels, the mass resolution on the finest level corresponds to a box of 256^3 particles. The realization of the initial spectrum of perturbations is done in such a way that this number of particles could be generated in the simulation box. The size of the simulation box is defined by the requirement of high mass resolution and by the total number of particles in the finest level. We set a box size of $15 h^{-1}$ Mpc on a side in all simulations which gives a mass per particle $m_p = 1.66 \times 10^7 h^{-1} M_\odot$ on the finest level of mass resolution. The omission of wavelengths larger than $15 h^{-1}$ Mpc may affect the characteristic mass and spatial distribution of halos, however, we do not expect it to influence the halo internal structure (Frenk et al. 1988). A host halo of about $2 \times 10^{12} h^{-1} M_\odot$ resimulated at high resolution will have more than 10^5 particles within its virial radius r_{vir} , defined as the radius at which the average halo density is 334 times the background density for our selected cosmology, according to the spherical top-hat model. Once the mass hierarchy is fixed, we start by running a low-mass resolution (LMR) simulation with 32^3 particles in a mesh with 256^3 cells from which potential host halos are to be identified for their future resimulation and analysis.

Second, the Bound Density Maxima (BDM) group finding algorithm (e.g., Colín et al. 1999) is used to locate potential host halos in the LMR simulation. The BDM algorithm finds the positions of local maxima in the density field smoothed at the scale of interest and applies physically motivated criteria to test whether a group of particles is a gravitationally bound halo. The friends of friends

⁴The number of mass levels was restricted by the amount of memory of the computer where the simulations were performed.

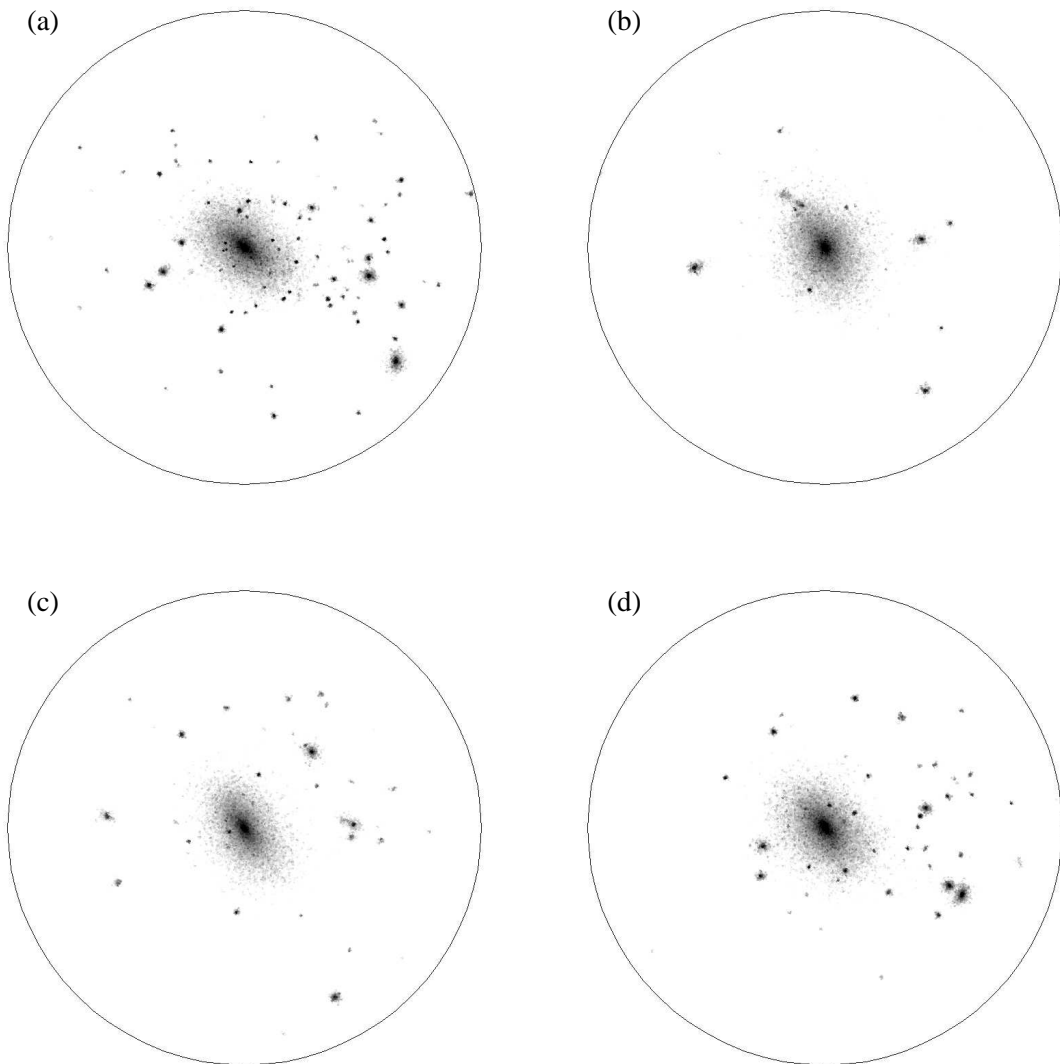


FIG. 1.— The distribution of dark matter particles inside a sphere of $400 h^{-1}\text{kpc}$ radius (solid circle) for the host halo II in four different models: (a) CDM model, and (b), (c), and (d) the WDM models with $R_{f,WDM} = 0.2, 0.1,$ and 0.05 Mpc, respectively. To enhance the contrast we have color-coded DM particles on a grey scale according to their local density (a pplot code kindly provided by A. Kravtsov) and removed all DM particles whose density was lower than a certain value. The local density at the particle positions was computed using SMOOTH, a publicly available code developed by the HPCC group in the UW Department of Astronomy.

group finding algorithm is then used on these halo population to identify the degree of isolation of each halo (halos are also visually located). Only halos which are relatively isolated⁵ were taken as potential host halos because we are interested in comparing our numerical results with the observed substructure in the Milky Way and Andromeda

galaxies (KKVP99; Moore et al. 1999a).

Third, we trace back all particles within a radius $r \gtrsim 1.5 r_{\text{vir}}$ of each selected host halo to get their lagrangian positions at $z = 40$. This radius is large enough to keep the contamination due to the presence of particles from the second mass level at the level of $\lesssim 1\%$ in mass. We then

⁵There are a couple of groups with a mass $\gtrsim 10^{13} h^{-1}M_{\odot}$ in our box. Milky Way-size halos belonging to one of these two groups were rejected for a subsequent analysis.

TABLE 1
STRUCTURAL PARAMETERS OF HOST HALOS

$R_{f,WDM}$ (Mpc)	Host halo name tag	V_{\max} (km/s)	M_{host} ($1 \times 10^{12} h^{-1} M_{\odot}$)	$N_{satellite}$	c_{NFW}	e_1	e_2	T
0.2	I	258	3.3	6	10.8	0.38	0.32	0.86
	II	246	3.1	7	9.4	0.22	0.19	0.87
0.1	I	270	3.4	13	12.0	0.41	0.29	0.76
	II	255	3.2	11	10.5	0.31	0.26	0.85
	III	241	2.1	4	10.2	0.34	0.14	0.47
	IV	196	1.7	13	7.6	0.41	0.26	0.69
0.05	I	271	3.5	15	12.6	0.45	0.35	0.83
	II	258	3.3	22	11.1	0.37	0.31	0.87
	III	246	2.1	13	13.9	0.34	0.18	0.58
0.0	II	263	3.3	35	11.0	0.36	0.34	0.96

regenerate the initial distribution using all particles with the four different weights (1, 8, 64, $512 \times m_p$). The farther away the particle is from the host halo the more massive the particle is. The simulation with $R_{f,WDM} = 0.1$ Mpc, for example, has 1,722,295 particles distributed as follows: 1,450,496 particles in the first-mass-level, 218,112 in the second-mass-level, and 31,040 and 22,647 in the third- and fourth-mass levels, respectively. The initial conditions are again evolved using ART with the capability of handling particles with different mass. The formal force resolution, measured by the size of a cell in the finest refinement grid, is $0.45 h^{-1} \text{kpc}$ and the number of time steps varies from 325 to 41600. Accurate results are expected at distances four times larger than the formal resolution.

Fourth, the BDM is used once again now to identify satellites (guest halos) orbiting around the center of mass of host halos. One of the parameters of BDM is the number of spheres that are randomly placed on the box to locate local maxima “seeds”. We made sure not to miss a significant fraction of guest halos by using the position of every fourteenth first-mass-level particle, a number which is much higher than the expected number of halos. For example, for the $R_{f,WDM} = 0.1$ Mpc model we used about 10^5 seeds. Some guest halos have been polluted by more than 5% in mass with particles from the second-mass level. These guest halos are usually at the periphery of the host halos and thus are more susceptible to being contaminated. We keep them in our satellite catalogs because we think they would still be there even if we increased the size of the high-resolution region. To measure the effect on the number of satellites due to the smallness of the high-resolution volume an additional simulation for one of the host halos—the halo II in the model with $R_{f,WDM} = 0.1$ Mpc—was run doubling the radius of the high-resolution region ($\sim 3 r_v$). The number of satellites within a sphere of radius $200 h^{-1} \text{kpc}$ centered on the host halo is equal to 11 in both simulations. This does not mean that there are not any differences at all; for example, a satellite, which was close to the center ($\sim 30 h^{-1} \text{kpc}$) in the simulation with the smaller high-resolution region, disappears in the test simulation. However, these differences are negligible as far as the cumulative circular velocity function for satellites is

concerned.

In Table 1 we present the values of some of the physical properties of the host halos re-simulated at high-resolution for each WDM model (i.e. for each selected $R_{f,WDM}$ value). The name tag of the host halo and its maximum circular velocity

$$V_{\max} = \left(\frac{GM(< r)}{r} \right)_{\max}^{1/2}, \quad (5)$$

where $M(< r)$ is the mass of the halo inside radius r , are placed in the second and third column, respectively. The virial mass and the number of satellites within a sphere of radius $200 h^{-1} \text{kpc}$, centered on the host halo, are displayed in the fourth and fifth column, respectively. All satellites with more than 10 bound particles are counted here. The concentration parameter c_{NFW} (Navarro, Frenk, & White 1997) is shown in the sixth column. It is defined here as the ratio between r_{vir} and r_s , where r_s is the NFW scale radius. Because our simulations possess the same seed we were able to identify a couple of host halos (I and II) in our three WDM models and make an inter-comparison study of their structural properties.

We have also measured the ellipticities of the host halos using the tensor of inertia. This is defined as

$$I_{i,j} = \sum x_i x_j / r^2, \quad (6)$$

where the sum is over all DM particles within r_{vir} , x_i ($i = 1, 2, 3$) are the coordinates of the particle with respect to the center of mass of the halo, and r is the distance of the particle to the halo center. The ellipticities are then given by

$$e_1 = 1 - \frac{\lambda_1}{\lambda_3}, \quad e_2 = 1 - \frac{\lambda_2}{\lambda_3}, \quad (7)$$

where $\lambda_3 > \lambda_2 > \lambda_1$ are the eigenvalues of the tensor of inertia. We evaluate the triaxiality parameter using the following formula (e.g., Franx, Illingworth, & de Zeeuw 1990)

$$T = \frac{\lambda_3^2 - \lambda_2^2}{\lambda_3^2 - \lambda_1^2} \quad (8)$$

A value of $T = 1.0$ means that the halo is prolate while a value of $T = 0.0$ represents an oblate halo. The ellipticities e_1 , e_2 , and the triaxial parameter for host halos are shown in the last three columns. The ellipticities increase as $R_{f,WDM}$ diminishes. In particular, the increment is by almost a factor of two for the host halo II when one goes from the WDM model with $R_{f,WDM} = 0.2$ Mpc to the CDM model.

Figure 1 provides a visual example of guest halos found in our different models, including a CDM model. As the host halo we have selected the one denoted by the roman number II in Table 1. This halo has a $V_{\max} \approx 250$ km/s but it varies a little from model to model. The letter (a) identifies the halo in the CDM model ($R_{f,WDM} = 0$) and letters from (b) to (d) represent the halo in WDM models from $R_{f,WDM} = 0.2$ Mpc to $R_{f,WDM} = 0.05$ Mpc, respectively. It is notable the absence of substructure and a greater roundness morphology of the host halo in our $R_{f,WDM} = 0.2$ Mpc model as compared with the CDM one, which agrees with the analysis of the host halos ellipticities of the previous paragraph.

4. THE CUMULATIVE CIRCULAR VELOCITY FUNCTION OF SATELLITES

The first interesting result that arises from our WDM simulations is that despite the power spectrum is suppressed below the free streaming scale, halos of size close to or smaller than $R_{f,WDM}$ are formed. This result is not obvious at all. Only high-resolution numerical simulations could show whether galactic substructures would form and survive in such a scenario with a filtered power spectrum at high wavenumbers. The number of satellites per host halo increases as $R_{f,WDM}$ decreases (see Table 1). This is in agreement with the numerical results at $z = 3$ of White & Croft 2000. Their cumulative number of halos above a certain mass increases as the cut-off wavenumber k_0 increases (the power spectrum suffers a sharp drop at k_0).

The present-day cumulative maximum circular velocity satellite functions, $N(> V_{\max})$, for our four models are displayed in Figure 2. These functions were estimated as follows: for each $R_{f,WDM}$ value we count the number of satellites with V_{\max} greater than a given value within $200 h^{-1}$ kpc from the center of host halos. This number is then divided by the number of host halos for each model and the volume of a sphere of $200 h^{-1}$ kpc radius. Although we plot this function down to $V_{\max} \sim 10$ km/s we are probably complete only to $V_{\max} \sim 20$ km/s (KKVP). As expected, the number of satellites is much smaller than the one predicted by a CDM model (KKVP; Moore et al. 1999a; Table 1 this paper). The WDM model that seems to reproduce better the observed $N(> V_{\max})$ function (taken from KKVP) is that with $R_{f,WDM} = 0.1$ Mpc or $m_w \approx 1$ keV. The discrepancy seen in Figure 2 between simulations and observations for $V_{\max} \gtrsim 50$ km/s can be attributed to the intrinsic dispersion of the mass aggregation history of host halos (Bullock, Kravtsov, & Weinberg 2000).

Is the reduced number of satellites at present time in the WDM scenario caused only by the suppression of power at small scales? To answer this question we counted the

number of guest halos in a sphere with proper radius $200 h^{-1}$ kpc centered on the host halo at $z = 1$, which is close to the nominal epoch of formation of host halos, and compared it with the number we have at $z = 0$. We did this only for the halo II⁶ for which a CDM simulation had also been performed. At $z = 1$ we obtain 29, 27, 20, and 10 guest halos for $R_{f,WDM} = 0, 0.05, 0.1, 0.2$ Mpc, respectively while at $z = 0$ the corresponding numbers are 28, 13, 9, and 4. Only halos with V_{\max} greater than 20 km/s were chosen and this lower limit on V_{\max} was increased by 20% for halos at $z = 1$ to take into account the evolutionary reduction of V_{\max} (e.g., Colín et al. 1999).

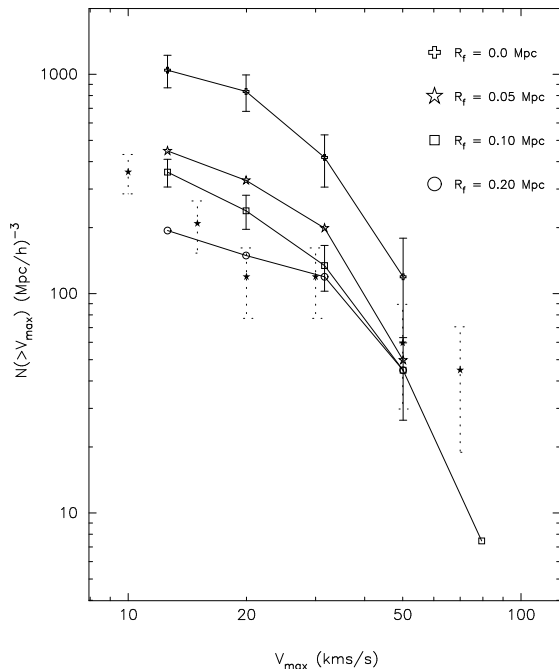


FIG. 2.— The cumulative maximum circular velocity V_{\max} function for satellites within $200 h^{-1}$ kpc from the center of the host halo. Solid lines represent the averaged V_{\max} function for each of our model, from top to bottom as $R_{f,WDM}$ goes from 0.0 to 0.2 Mpc. The averaged V_{\max} function from satellites of Milky Way and Andromeda is represented by stars (taken from KKVP). Error bars are just Poisson errors. For clarity, we only plot error bars for the CDM model and the WDM model with $R_{f,WDM} = 0.1$ Mpc and the observed V_{\max} function is displayed with dotted error bars. The square at $V_{\max} \sim 80$ km/s has no error bar because there is only one guest halo at this bin.

The number of guest halos for the CDM model remains approximately constant within this proper volume after $z = 1$ (Moore et al. 1999a). Does this mean that the guest halos inside this volume are not destroyed and that small halos outside this volume do not fall later into this volume? We have done the following experiment to measure the degree of satellite destruction (Kravtsov 2000): we have tagged all DM particles within $200 h^{-1}$ kpc from the center of the host halo at $z = 0$ and traced back them at $z = 1$. We then apply the BDM algorithm on this subset of DM particles at $z = 1$. The difference between the

⁶The BDM algorithm finds two progenitors of the host halo I of comparable mass at $z = 1$, so we decided not to use this halo for the argument developed in the paragraph.

number of halos found at $z = 1$ and its number at $z = 0$ gives us the degree of satellite destruction. The percentage of destruction is about 35% for the CDM model while it is 63% for the WDM model with $R_{f,WDM} = 0.1$ Mpc. Since there is indeed destruction of guest halos from $z = 1$ to $z = 0$, the only manner to maintain a constant number of satellites in the CDM model is by incorporating small halos from outside the chosen volume (actually, some small halos might also form within the volume; however, the probability of such an event is very low). The accretion rate of guest halos is less in the WDM models just because the number of available halos that could fall into the volume is lower than in the CDM case. We have also detected that guest halos are more easily destroyed in the WDM models. These two effects which are of comparable size work together to deliver a much smaller number of satellites at $z = 0$.

The more efficient disruption of satellites in the WDM scenario is very likely due to the fact that guest halos are less concentrated in this scenario (see next section). In fact, we have found that the guest halos that survived until $z = 0$ are more concentrated than those at $z = 1$. On average, the guest halos at $z \approx 1 - 1.5$ are twice less concentrated than those at $z = 0$.

5. CONCENTRATIONS AND DENSITY PROFILES

We define the concentration parameter $c_{1/5}$ as the ratio between the halo radius r_h ⁷ and the radius within which 1/5 of the total halo mass M_h is contained. In Figure 3 we plot this parameter versus the halo mass for host (large symbols) and guest (small symbols) halos for our WDM model with $R_{f,WDM} = 0.2$ Mpc (triangles) and the CDM model (crosses). Only those halos which have more than 90 particles inside their radii have been analyzed. The solid and dashed lines in Figure 3 are extrapolations to small masses of the relations $c_{1/5} - M_h$ found by Avila-Reese et al. (1999) for the corresponding CDM model for isolated halos and halos in groups, respectively. From Figure 3 one can see that the concentration of host WDM halos is only slightly smaller than that of CDM halos. For the small guest halos, the difference is more notable; in the $10^9 - 10^{11} h^{-1}M_\odot$ mass range the concentrations for the case $R_{f,WDM} = 0.2$ Mpc are approximately 1.8 – 1.2 times smaller than those obtained in the CDM model. It is interesting to see that the extrapolations showed in Figure 3 do actually agree with the concentrations of the guest halos in our fiducial CDM model.

The density profiles of host halos obtained in our simulations with $R_{f,WDM} = 0.2, 0.1, 0.05,$ and 0.0 Mpc ($M_h \approx 1 - 3 \times 10^{12} h^{-1}M_\odot$) are shown in Figure 4 (symbols). In order to avoid overlapping, the profiles from the $R_{f,WDM} = 0.1, 0.05,$ and 0.0 Mpc models were shifted in $\log \rho$ by $-1, -2,$ and $-3,$ respectively. These density profiles are well described by the NFW formula (lines), although the inner slope in some cases of the WDM models is slightly shallower than r^{-1} . The inner profile for the CDM halo is actually steeper than r^{-1} . The corresponding NFW concentration parameters for the host halos are given in Table 1. For comparison, in the CDM simulation of Avila-Reese et al. 1999 a $10^{12} h^{-1}M_\odot$ halo has in

average $c_{NFW} \approx 12$.

The guest halos ($M_h \approx 10^9 - 10^{11} h^{-1}M_\odot$) present a wide diversity of density profiles. Unfortunately, since the number of particles in these halos is not very large ($\sim 100 - 200$ particles for most of them), the resolution is not sufficient to study the inner density profile with accuracy (see a discussion on this subject in §6.2). For those guest halos ($\sim 15\%$) whose density profiles are reasonably well described by the NFW fit we obtain a mean $c_{NFW} \approx 8$ and 10 for $R_{f,WDM} = 0.2$ and 0.05 Mpc models, respectively. We estimate a mean c_{NFW} of 25 by extrapolating the results of the CDM model to low masses (Avila-Reese et al. 1999) or by using our own CDM simulation.

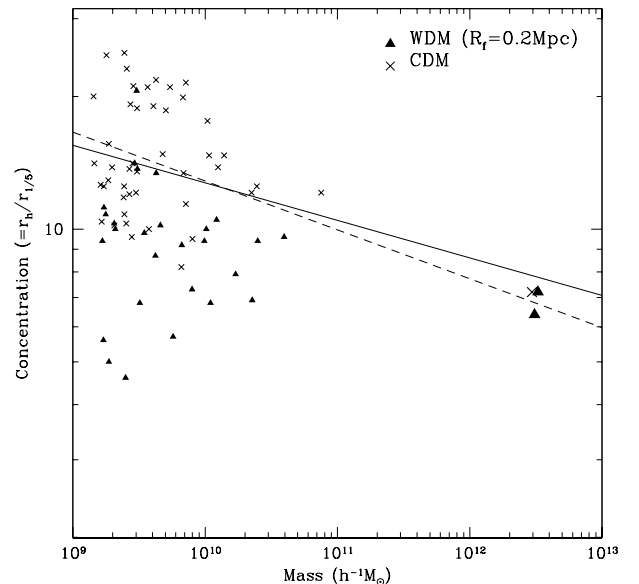


FIG. 3.— The concentration parameter $c_{1/5}$ versus the mass for host halos (large symbols) and guest halos with more than 90 particles (small symbols) in the WDM ($R_{f,WDM} = 0.2$, solid triangles) and CDM (crosses) simulations. The solid and dashed lines correspond to the linear fittings found in a CDM simulation for isolated halos and halos within group- and galaxy-size halos, respectively (Avila-Reese et al. 1999). The only host CDM halo here resulted less concentrated than the average.

6. DISCUSSION

6.1. The accretion and destruction rates of guest halos

Our results show that in a WDM model with $R_{f,WDM} = 0.1$ Mpc the number of guest halos within Milky Way-size halos agrees with the observed number of satellites in the Milky Way and Andromeda galaxies. Using the extended Press-Schechter formalism and assuming that *the amount of substructure is preserved since the host halo formation epoch*, Kamionkowski & Liddle (1999) also found good agreement with the observations for models with a sharp drop in the power spectrum on small scales and with zero velocity dispersion (they were interested in studying the broken-scale-invariant model). However, the

⁷The halo radius r_h is defined as the minimum between r_{vir} and the truncation radius (where the spherically averaged outer density profile flattens or even increases). In fact, all the host halos and most of the guest halos (more than 70%) attain their virial radius.

cut-off length-scale in the power spectrum they required is two to three times smaller than the one used here in order to fit the observational data. We argue that at the basis of this difference is the fact that for models with a cut-off in the power spectrum and with negligible particle dispersion velocities, the amount of substructure in a host halo *is not* preserved.

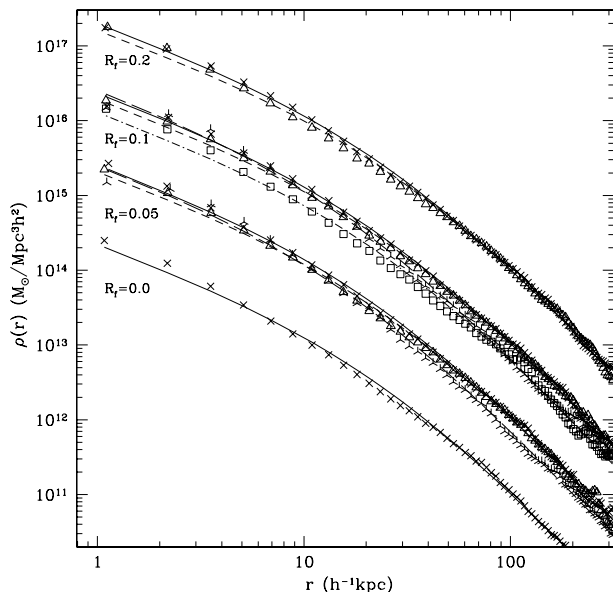


FIG. 4 The density profiles of the host halos in the WDM models with $R_{f,WDM} = 0.2, 0.1$ and 0.05 Mpc, and in the CDM model ($R_{f,WDM} = 0.0$). The profiles of the three latter simulations were shifted in the log of the density by $-1, -2,$ and -3 in order to avoid overlapping. The different lines are fits to the data using the NFW profile and have the same correspondence with the symbols in each one of the models. The corresponding NFW concentration parameters are given in Table 1.

In Section 4, we have shown that for the CDM model the number of satellites within a sphere of proper radius $200 h^{-1} \text{kpc}$ centered on the host halo remains approximately constant from the nominal epoch of host halo formation up to the present time (see also Moore et al. 1999a). Nevertheless, as discussed in § 4, this is a particular case in which the destruction and accretion/formation rates of guest halos balance up. In WDM models, the accretion/formation rate of guest halos is smaller and the destruction rate is more efficient than the one in the CDM scenario. These two facts operate at the same time to produce a number of guest halos at $z = 0$ much smaller than the one found at the nominal epoch of host halo formation. Therefore, Kamionkowski & Liddle (1999) overestimated the filtering scale of the power spectrum because they did not consider that a high fraction of satellites are destroyed by dynamical effects during their lifetime in the dense environment of host halos. Recently, White & Croft (2000) have reported from numerical simulations of WDM models that at $z = 3$ the number of small halos is reduced roughly by a factor of five when the CDM spectrum is filtered at scales much larger than 0.1 Mpc. If one takes into account that

a significant fraction of these halos will be destroyed by $z = 0$ and not many small halos will be accreted, then the agreement with observations will be reached for a cut-off scale smaller than the one suggested by these authors.

Why a significant fraction of guest halos become destroyed in the WDM scenario? We offer the following answer: in a WDM model these halos form later than in a CDM model, when the mean density of the universe was lower. For example, the formation redshift (defined as the redshift where $\sigma(M_{\text{vir}}, z) = 1$) of a halo of $M_{\text{vir}} = 2 \times 10^9 h^{-1} M_{\odot}$ is 4.1 for the CDM model, whereas for the WDM model with $R_{f,WDM} = 0.2$ Mpc it is 2.5. Thus, the characteristic overdensity δ_c for guest halos of this mass in this WDM model is about 4.5 lower than the corresponding for guest halos in the CDM model. If δ_c approximately scales as the cube of the concentration parameter, this would mean that these halos were about 1.7 less concentrated at their formation epoch. This interpretation agrees with the results from our study on concentration parameters (§5). In summary, guest halos in WDM models are more easily disrupted because of their puffier density distribution

6.2. Density profiles of the WDM halos

We have found that the present-day density profiles of Milky Way-size galactic halos in a WDM model with a $R_{f,WDM}$ value corresponding to masses of the order of a few $10^9 M_{\odot}$ do not differ from those obtained in CDM models. A similar result was also reported by Moore et al. (1999b). They cut the power spectrum on a mass scale smaller by more than a factor of ten than the mass of the studied cluster. The question about how the filtering of the power spectrum affects the inner density profiles of halos with masses close or smaller than the cut-off mass scale is still open (see Avila-Reese et al. 1998). Unfortunately, we could not explore this question in detail in this paper because our guest halos with masses close to $2 \times 10^9 M_{\odot}$ are poorly resolved (a study on this direction is in progress; small halos in a WDM cosmology are being resimulated with high-resolution). Nevertheless, we have found that the small WDM halos are actually less concentrated than the CDM ones. The difference in the mean in our extreme $R_{f,WDM} = 0.2$ Mpc model is less than a factor of two in the $c_{1/5}$ parameter. We estimate that this factor is too small to offer a solution to the problem related to the inner structure of dwarf galaxy dark halos. Thus, although the WDM scenario helps, apparently it does not solve this problem. Nevertheless, some questions that remain open might change this conclusion. In the following, we discuss them.

In the monolithic collapse the orbital tangential velocity of the collapsing particles plays a significant role in the final virialized configuration; it is expected that in a hot monolithic collapse shallow cores form (e.g., van Albada 1982; Aguilar & Merrit 1990; Firmani et al. 2000b). To produce a hot monolithic collapse in a cosmological scenario, dark matter particles should have a non-negligible velocity dispersion (thermal energy) at the redshift of the halo formation — there should also be a cut-off in the power spectrum at the scale of interest. On the other hand, if this is the case, then the formation of shallow cores with a maximum limiting density determined by the velocity dispersion is expected (Hogan & Dalcanton 2000). These

authors estimate that shallow cores, which are in agreement with observational determinations in dwarf galaxies, can be produced if warmons have a mass $m_W \approx 200$ eV; in this case the particle dispersion velocity is significant. Of course, according to our results, a WDM model with $m_W \approx 200$ eV would produce too few guest halos to agree with observations. However, if the inclusion of gas within the guest halos plays an important role to avoid their disruption, then a larger fraction of guest halos could survive until the present epoch. It is probable that with an m_W only slightly smaller than 1keV, shallow cores that explain the rotation curves of dwarf galaxies form if the velocity dispersion is taken into account. Nevertheless, as we have shown, in this case shallow cores in the massive (host) halos will not be produced. Thus, if the increment of the core radius with the halo mass or V_{\max} inferred by Avila-Reese et al. (1998) and Firmani et al. (2000b) from observations is confirmed, then the collisionless WDM scenario is ruled out. It is interesting to note that in a self-interacting WDM model, the particle velocity dispersion would be larger than in the collisionless case (Hannestad & Scherrer 2000). A detailed numerical study of this model, which appears to be more palatable than a self-interacting CDM model, is desirable.

Finally, we should comment that the problem of an apparently excessive number of guest halos in the CDM model holds if one assumes that each guest halo hosts a luminous galaxy. This assumption was recently challenged by Bullock et al. (2000) who proposed that reionization can efficiently inhibit dwarf galaxy formation.

7. CONCLUSIONS

Using high-resolution N-body simulations, we have studied the substructure inside Milky Way-size halos in a WDM cosmological scenario. We have also addressed the question whether the density profiles of host and guest halos are different from their corresponding CDM ones. Our main conclusions are:

1. Despite the fact that the power spectrum of fluctuations is suppressed at small scales, a non-negligible number of virialized structures, corresponding to these or smaller scales, form and survive within larger structures. The accretion rate of small halos is found to be less in the WDM scenario than in the CDM one. This is simply explained by the fact that a smaller number of small halos are available for their incorporation into host halos in the WDM models. A higher satellite destruction rate is found in the WDM scenario as compared with the one in the CDM model: it can be accounted for the fact that guest halos are less concentrated by about a factor two in average in the WDM models. The less efficient halo accretion and the higher satellite destruction have almost the same weight as far as the final count of satellites within host halos at $z = 0$ is

concerned. The larger the $R_{f,WDM}$ value the greater the size of these two effects, and the smaller the abundance of satellites.

2. The predicted maximum circular velocity function of guest halos that seems to best fit the observed one for satellites in the Milky Way and Andromeda is that given by the $R_{f,WDM} = 0.1$ Mpc model. This $R_{f,WDM}$ value corresponds to a warmon of mass about 1 keV.

3. For the $R_{f,WDM} = 0.1$ and 0.2 Mpc models, guest halos ($M_h \approx 10^9 - 10^{11} h^{-1}M_\odot$) have a concentration parameter $c_{1/5}$ which is roughly twice smaller than that of the CDM halos. For those guest halos whose density profiles are reasonably well described by a NFW parametric fit ($\sim 15\%$), the c_{NFW} parameter is roughly 1.5 – 3.0 times lower than that of the CDM halos. This difference in the concentration parameters, for both $c_{1/5}$ and c_{NFW} , vanishes as we go to more massive halos.

4. The density profile of the host halos ($M_{\text{vir}} \approx 1 - 3 \times 10^{12} h^{-1}M_\odot$) is well described by the NFW profile (in some cases, the inner slope is slightly shallower than r^{-1}). The guest halos have a wide variety of density profiles and those whose masses are below the corresponding cut-off mass scale probably present a small shallow core. The poor mass resolution of the simulations at these scales limits our predictions.

In summary, we have shown that in the WDM model with $R_{f,WDM} \approx 0.1$ Mpc or $m_W \approx 1$ keV the degree of substructure within a Milky Way-size halo is much lower than in the CDM model and is in agreement with observations, if one assumes that each guest halo hosts a luminous galaxy. The problem of cuspy halos probably still persists in the WDM scenario, although we have found that halos—in particular the small ones—are less concentrated than the corresponding CDM halos. If the inclusion of baryonic matter helps to significantly avoid disruption of substructure, then the agreement with observation may continue for less massive WDM candidates for which the rms velocity is larger. In this case, the formation of shallow cores in dwarf galaxy like halos is expected. Nevertheless, as we have shown, halos of larger masses will not have a shallow core.

We are grateful to Anatoly Klypin and Andrey Kravtsov for kindly providing us a copy of the ART code in its version of multiple mass, and for enlightening discussions. We also acknowledge the anonymous referee whose helpful comments and suggestions improved some aspects of this paper. P. C. and V.A. acknowledge the hospitality of the NMSU Astronomy Department. Our ART simulations were performed at the Dirección General de Servicios de Cómputo Académico, UNAM, using an Origin-2000 computer.

REFERENCES

- Aguilar, L., Merritt, D. 1990, ApJ, 354, 33
 Avila-Reese, V., Firmani, C., & Hernández, X. 1998, ApJ, 505, 37
 Avila-Reese, V., Firmani, C., Klypin, A., & Kravtsov, A.V. 1999, MNRAS, 310, 527
 Bardeen, J.M., Bond, J.R., Kaiser, N., & Szalay, A.S. 1986, ApJ, 304, 15
 Binney, J., Gerhard, O., & Silk, J. 2000, MNRAS submitted (astro-ph/0003199)
 Bullock, J. S., Kravtsov, A.V., & Weinberg, D.H. 2000, ApJ, submitted (astro-ph/0002214)
 Burkert, A. 1995, ApJ, 477, L25
 Burkert, A. 2000, ApJ submitted (astro-ph/0002409)
 Carlberg, R.G., Yee, H.K.C., Ellingson, E., Abraham, R., Gravel, P., Morris, S., Pritchet, C.J. 1996, ApJ, 462, 32
 Colín, P., Klypin, A.A., Kravtsov, A.V., & A.M. Khokhlov. 1999, ApJ, 523, 32
 Colombi, S., Dodelson, S., & Widrow, L.M. 1996, ApJ, 458, 1

- Cowsik, R., & McClelland, J. 1972, *PhRvL* 29, 669
- de Blok W.J.G., & McGaugh S. S., 1997, *MNRAS*, 290, 533
- Eke, V.R., Cole, S., Frenk, C.S., & Henry, P.J. 1998, *MNRAS*, 298, 1145 1996, *ApJ*, 462, 32
- Gelato, S., & Sommer-Larsen, J. 1999, *MNRAS*, 303, 321
- Firmani, C., & Avila-Reese, V. 2000, *MNRAS* in press ([astro-ph/0001219](#))
- Firmani, C., D'Onghia, E., Avila-Reese, V., Chincarini, G., & Hernández, X. 2000a, *MNRAS* in press ([astro-ph/0002376](#))
- Firmani, C., D'Onghia, E., Chincarini, G., Hernández, X., & Avila-Reese, V. 2000b, *MNRAS*, submitted ([astro-ph/0005001](#))
- Flores, R., & Primack, J.R. 1994, *ApJ*, 427, L1
- Franx, M., Illingworth, G., & de Zeeuw, T. 1990, *ApJ*, 383, 112
- Frenk, C.S., White, S.D.M., Davis, M., & Efstathiou, G. 1988, *ApJ*, 327, 507
- Hannestad, S. 1999, preprint ([astro-ph/9912558](#))
- Hannestad, S. 2000, preprint ([astro-ph/0003046](#))
- Hernández, X., & Gilmore, G. 1998, *MNRAS*, 294, 595
- Hogan, C.J., & Dalcanton, J.J. 2000, preprint ([astro-ph/0002330](#))
- Kamionkowski, M., & Liddle, A.R. 1999, preprint ([astro-ph/9911103](#))
- Kauffmann, G., White, S. D. M., & Guideroni, B. 1993, *MNRAS*, 264, 201
- Klypin, A.A., Kravtsov, A.V., Valenzuela, O., Prada, F. 1999, *ApJ*, 522, 82 (KKVP)
- Klypin, A.A., & Holtzman, J. 1997, preprint ([astro-ph/9712217](#))
- Klypin, A.A., Kravtsov, A.V., Bullock, J., & Primack, J. 2000, in preparation
- Kolb, E.W., & Turner, M.S. 1990, *The Early Universe* (Redwood City: Addison-Wesley)
- Kravtsov, A.V. 2000, private communication
- Kravtsov, A.V., Klypin, A.A., & Khokhlov, A.M. 1997, *ApJS* 111, 73
- Mo, H.J., & Mao, S. 2000, *MNRAS* submitted ([astro-ph/0002451](#))
- Mohr, J.J., Mathiesen, B., & Evrard, A.E. 1999, *ApJ*, 517, 627
- Moore, B. 1994, *Nature*, 370, 629
- Moore, B., Ghigna, S., Governato, F., Lake, G., Quinn, T., Stadel, J., & Tozzi, P. 1999a, *ApJ*, 524, L19
- Moore, B., Quinn, T., Governato, F., Stadel, J., & Lake, G. 1999b, *MNRAS*, 310, 1147
- Moore, B., Gelato, S., Jenkins, A., Pearce, F.R., & Quilis, V. 2000, *ApJ* submitted ([astro-ph/0002463](#))
- Navarro, J.F., Eke, V.R., & Frenk, C.S. 1996, *MNRAS*, 283, L72
- Navarro, J.F. 1998, *ApJ* submitted ([astro-ph/9807084](#))
- Navarro, J.F., & Steinmetz, M. 1999, *ApJ* in press ([astro-ph/9908114](#))
- Navarro, J.F., Frenk, C.S., & White, S.D.M. 1997, *ApJ*, 490, 493
- Nevalainen, J., & Roos, M. 1998, *A&A*, 339, 7
- Peebles, P.J.E. 2000, preprint ([astro-ph/0002495](#))
- Peacock, J., & Dodds, S. 1994, *MNRAS* 267, 1020
- Perlmutter, S. et al. 1999, *ApJ*, 517, 565
- Riess, A.G. et al. 1998, *AJ*, 116, 1009
- Riotto, A., & Tkachev, I. 2000, preprint ([astro-ph/0003388](#))
- Schmidt, B.P. et al. 1998, *ApJ*, 507, 46
- Sommer-Larsen, J., & Dolgov, A. 2000, *ApJ* submitted ([astro-ph/9912166](#))
- Spergel D.N., & Steinhardt P.J. 2000, *Phys.Rev.Lett.*, 84, 3760
- Swaters, R.A., Madore, B.F., & Trewella, M. 2000, *ApJ* in press ([astro-ph/0001277](#))
- Tyson J.A., Kochanski G.P., & Dell'Antonio I.P. 1998, *ApJ*, 498, L107
- van Albada, T.S. 1982, *MNRAS*, 201, 939
- van den Bosch, F., Robertson, B.E, Dalcanton, J.J., & de Blok, W.J.G. 1999, *AJ* submitted ([astro-ph/9912004](#))
- Yoshida, N., Springel, V., White, S.D.M., & Tormen, G. 2000, *ApJ* submitted ([astro-ph/0002362](#))
- White, M., & Croft, R.A.C. 2000, preprint ([astro-ph/0001247](#))